Jerzy Nowacki, Norbert Sieczkiewicz, Michał Nocoń

The Use of 3D Scanning Technology in Measurements of Welding Distortions

Abstract: The article describes primary issues related to measurements of welding distortions performed using 3D scanning methods. The study includes a review of available industrial 3D scanning solutions. The research involved the experimental investigation of high-strength steels containing welding distortions as well as the SAW surfacing of steel S960QL steel performed using various welding parameters. The research-related tests included the selection of an appropriate 3D scanning technology. During the tests, steel plates were measured using GOM ATOS III Triple Scan and 3D scans were obtained using Kinect for Windows v1 and v2, DAVID SLS-3. The research results demonstrated that the choice of a metrology-grade 3D scanner used for measurements of weld distortions ensured the obtainment of required accuracy of measurements.

Keywords: welding distortions; 3D scanning; structured light scanning; laser scanning

DOI: *10.17729/ebis.2019.1/3*

Introduction

A heat input to a joint during welding and surfacing is responsible for a significant temperature gradient as well as for the formation of thermal stresses and strains. The unpredictable (entirely) nature of welding strains and a gap in the exact theoretical or experimental criteria of welding strain prediction increase the significance of effective measurement techniques and strain analysis. The 3D scanning-based tests discussed in the article aimed to compare and select the optimum scanning technique as well as the performance of measurements and the comparison of strains in specimens made of steel S960QL subjected to surfacing performed using various parameters.

Selected 3D scanning techniques

Short-range laser scanners

Short-range laser scanners are used for triangulation enabling the recording of a 3D object shape and its description (in the form of a point cloud). The laser beam is directed onto the surface of an object. After being reflected against the scanned surface, the initial beam trajectory is disturbed and collected in the CCD optical sensor. Based on the disturbed beam, triangulation makers it possible to identify the angle of light reflection, depending on the distance between the scanner and the test surface (and being the basis for calculating the distance

prof dr hab. inż. Jerzy Nowacki (Professor PhD (DSc) Habilitated Eng.); mgr inż. Norbert Sieczkiewicz (MSc. Eng.), mgr inż. Michał Nocoń (MSc. Eng.) – West Pomeranian University of Technology in Szczecin, Institute of Materials Engineering

between the scanner and the object). Once the scanner has collected the sufficient amount of data, it is possible to create the map and an object subjected to scanning. To ensure the proper scanning of an object, the distance between the sensor and the laser radiation source must be known and strictly specified. The advantages of short-distance laser scanners include accuracy, resolution, portability and lower sensitivity to changing light conditions, e.g. in comparison with photogrammetric methods. Because of the fact that short-distance scanners are not very useful in relation to transparent or glossy surfaces, such surfaces need to be tarnished before being scanned by the above-named scanners [1,2].

Long-distance scanners

Long-distance scanners include pulsed scanners and phase shift scanners. Because of higher precision, triangulation-based scanners are used for shorter distances (Table 1).

Pulsed scanners

Because of high impulse power and the short time of an impulse, pulsed scanners are useful in long-distance scanning. Pulsed scanners measure the distance between an object and a sensor on the basis of a time necessary for the laser beam to reach the object and return to the sensor. Collected data are processed by a set of electric circuits enabling the determination of time after which laser light returns to the sensor with an accuracy of a picosecond. When using pulsed lasers, during one measurement it is possible to identify the position of just one point, therefore, in order to scan a 3D surface, the laser must perform full rotation (360 degrees). The full rotation is obtained using a mirror changing the direction of the laser beam. A significant advantage of pulsed scanners is the possibility of scanning large objects, whereas their limitation is the low rate of scanning [2, 4].

Phase-shift scanners

Similar to pulsed laser scanners, phase-shift scanners are characterised by the possibility of changing the power of laser radiation and emitting the beam of variable amplitude. A difference in the phase of the emitted and reflected beam constitutes the basis for the estimation of the time of delay and distance. Because of determining the distance on the basis of an impulse passage time and phase shift, phase-shift scanners are more precise than pulsed scanners, yet are also characterised by greater limitations in

Table 1. Metrological characteristics of laser scanning techniques [3]

Measurement technique	Measurement range, m	Accuracy, mm	Measurement rate, points per second
Measurement of impulse passage time	<1500	<20	up to 12 000
Measurement of phase shift	<100	<10	up to 625 000
Triangulation	a few metres	<0.1	up to 10 000

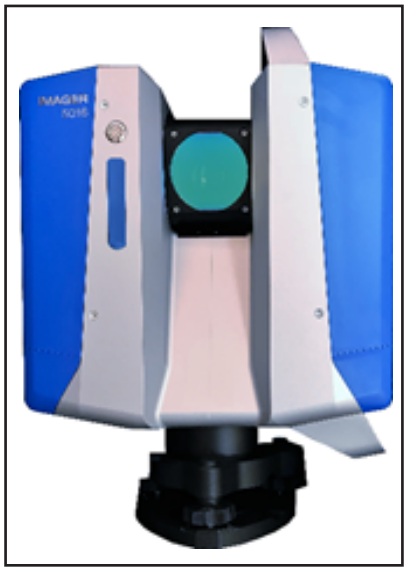

Fig. 1. Z+F IMAGER 5016 3D laser scanner with the maximum range of up to 360 meters

Fig. 2. Omnitrac 2 wireless laser tracker (Automated Precision); spherically mounted retroreflectors having a diameter of 0.5 inch used in pair with additional tooling (pin nest adapter)

terms of range [1, 4]. An example of the aforesaid scanner, i.e. where the distance is measured on the basis of a difference in the laser beam phase, is an Z+F Imager 5016 industrial scanner (Fig. 1) and an Omnitrac 2 laser tracker (Fig. 2), enabling the scanning of large objects at predefined points. Information concerning the coordinates of a given point is obtained by comparing the phases of the beam emitted by the head and reflected against an object as well as from two encoders providing information about rotations of the head in two planes [5]. The Z+F Imager 5016 scanner is characterised by a significant scanning range of up to 360 metres [9]), making it a competitive alternative to pulsed scanners.

Scanners emitting structured light

Scanners emitting structured light are based on blue or white LED light, which can be emitted both by the LCD and the DLP projector. Scanners based on structured light project a series of linear light models on an object. The shape of the object is detected by one or two cameras through the deformation of the model. The software is capable of distinguishing edges of each line in the model and, on the basis of triangulation, to identify the distance of each tested surface from the scanner and to determine the shape of the object [9]. In cases of systems based on two cameras, two images are obtained per a scan, making it possible to create a 3D image in one take. The scanners are characterised by high resolution and a significant scanning rate making it possible to perform a single scan within 2 seconds. In contrast with laser scanners, structured light-based scanners are safe for eyesight. However, as regards objects of complex geometry, the scanners are disadvantaged by the necessity of making scans at various angles to fully scan a given object. In addition, the above-named scanners are sensitive to the surrounding light and should not be used in field conditions. Sensitivity to the environment can be partly reduced by using scanners provided with a projector emitting blue light. Examples of industrial structured light optical scanners are a Gom Atos Triple Scan (Fig. 4) and Atos Core (Fig. 3). Measurements can be carried out manually by placing the scanner on the stand or the desktop. In addition, the scanner can constitute an optical component of a fully automated measurement machine (manufactured by Gom), where a photogrammetric scanner can be placed on the Triple Scan scanner for better reproducibility and uniform accuracy within the entire scanning area. The aforesaid advantages result from improved positioning based on reference points. The Atos Triple Scan scanner uses blue LED light as the light source; images are recorded using stereoscopic cameras [1, 7]. Alternative solutions are Comet systems manufactured by the Zeiss company.

Fig. 3. GOM ATOS ScanPort - an optical desktop scanner equipped with the automated rotating table

Manual portable scanners

An innovation in portable scanners consists in their positioning system. In contrast to other solutions, utilising the physical connection with the scanner to identify its position or optical systems in an external tracking device monitoring the position of a scanner, portable scanners use the self-positioning system. This can be based on natural characteristic points

contained in the geometry of an object subjected to scanning or on the basis of reference points. Both solutions utilise two cameras in order to create the stereoscopic vision of the scanner system. When the position of the scanner is changed, the position of the scanner in relation to the object being scanned is determined on the basis of the triangulation in relation to reference points or characteristic points of the object geometry. The positioning based on reference points makes it possible to collect data regardless of the surface of the object being scanned. In the above-named case, the total scanning time is longer because of the necessity of placing points on the object and defining them initially, yet the accuracy of scanning is higher (comparable with that obtainable using the measurement arm). Measurement points, usually circles (because of their easy detectability by the optical elements of the scanner) should be applied before scanning. In addition, to obtain accurate results, the object should be initially described (through the individual detection of reference points by the scanner). The subsequent stage involves the identification of the relative position; each scan frame requires a minimum of 3 reference points. The movement of the scanner is accompanied by the recognition of successive three points and their recording in the global positioning system. The second positioning method utilises object characteristics, i.e. design and shape, to position the object in space. To identify the appropriate position of the scanner, subsequent scan frames are analysed on the basis of the comparison of the object shape on an already recorded image. This positioning method significantly facilitates and quickens the scanning process, yet it has certain disadvantages. In contrast to reference points, natural reference points may vary significantly depending on an object being scanned, which affects scanning accuracy. Bodies of revolution, e.g. a cylinder, usually have overly few characteristic points for the above-named positioning method to scan the object successfully. It is possible to combine the two above-presented methods into a one hybrid method. If there are not enough characteristic points on the object, reference points can be placed on areas lacking characteristic points. Regrettably, when using the hybrid method it is not possible to obtain scanning accuracy characteristic of the method based on a large number of reference points. The second method involves the use of accelerometers and gyroscopes built-in in the self-positioning scanner. In the latter case, the scanner identifies its position on the basis of accelerations and angles of rotation. The aforesaid solution reduces sensitivity in relation to the object geometry and does not require the placing of reference points, additionally reducing the time of scanning. Manual portable scanners are based on the laser technology and on the white light technology. The principle of scanner operation is similar to that of laser scanners or white light-based scanners, where light or laser distortions are analysed in order to obtain a 3D model. The greatest advantage of portable manual scanners is their handiness and simplicity of operation in comparison with other types of scanners. In addition, portable manual scanners can generate 3D images on a real-time basis (during scanning). Because of the innovative positioning system, it is possible to scan objects in poorly accessible spaces/areas and provide the operator with the freedom of movements. [6, 8]

3D scanning of welding distortions

The identification of the usability of 3D scanning in the analysis of welding distortions involved the scanning of square specimens (Fig. 4) made of steel S960QL, before and after submerged arc surfacing. During the process of surfacing (Table 2), the surfacing rate was constant (in all of the tests) and amounted to 40 cm/min. Afterwards, the mesh after surfacing was analysed (compared) using the CAD model CAD (generated on the basis of the mesh before surfacing) and the coloured maps of deviations were obtained.

Table 2. Parameters used in the surfacing of the steel specimens

Specimen no.	Current, A		Voltage, V	Heat input, kJ/mm
1	350		25	1.31
2	400		25.5	1.53
3	450		26	1.76
4	350		25	1.31
5	400		25.5	1.53
6	450		26	1.76
7	450		30	2.03
8	450		30	2.03
9	450		30	2.03
10	1 run	450	30	2.03
	2 run	500	30	2.25

Measurement system and its configuration

The scanning of the specimens was performed using a Gom Atos ScanBox 6 series machine. The Atos ScanBox is composed of the following elements:

- Fanuc M-10iA industrial robot,
- 3D Gom Atos III Triple Scan structured scanner,
- measurement cell,
- rotating table.

The Gom Atos III Triple Scan has variable measurement spaces ranging from 38 mm × 29 mm × 15 mm to 2000 mm × 1500 mm × 1500 mm. The measurement field selected for the specimens having the length of their side amounting to 176 mm had the dimensions of 320 mm × 240 mm × 240 mm [9]. As recommended by the manufacturer of the Gom scanner, in relation to a given size of the field, the specimens were provided with index points having diameter of 1.5 mm each. The black areas of the points were gently captured using tweezers (not to damage the geometry of the points) and next applied on the specimen. Because of the fact that the points were made in a high tolerance class, any damage to them might affect measurement results.

Pretreatment of the surface

Before scanning, all impurities were removed from the specimens using extraction naphtha. As the surface of the specimens was homogenous and mat, scanning was performed without the covering of the surface with white paint. One specimen, characterised by the greatest reflections, was first scanned without tarnishing the surface and, next, after tarnishing the surface using Helling Standard-Check no. 3 spray (Fig. 5). The tarnishing improved the quality of scanning, i.e. the smaller number of holes in the polygonised model.

The result obtained without tarnishing the specimen was sufficient to perform scanning. Skipping the tarnishing process made it possible to reduce time necessary for the performance of the test and helped avoid difficulty determining the thickness of marker coating, potentially affecting measurement results (Fig. 6).

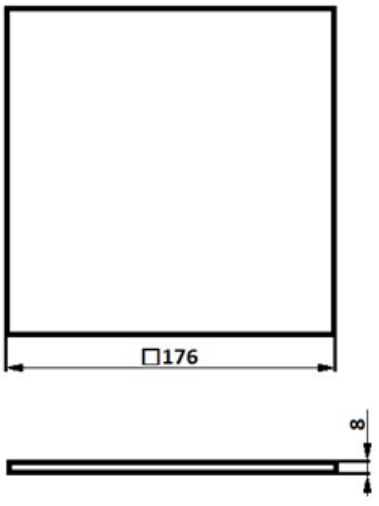

Fig. 4. Dimensions of the specimen

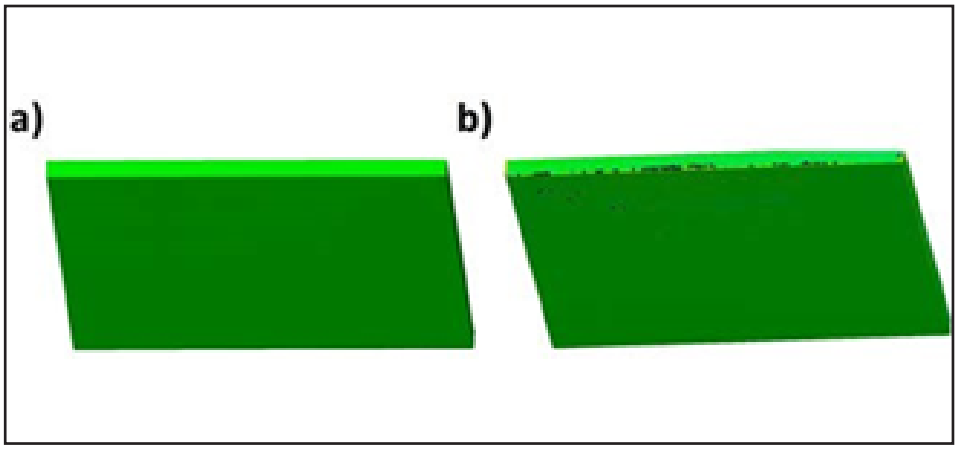

Fig. 5. Object: a) surface coated with the Helling Standard-Check no. 3 spray (reducing and removing reflections – tarnish effect), b) object not subjected to pretreatment (visible reflections)

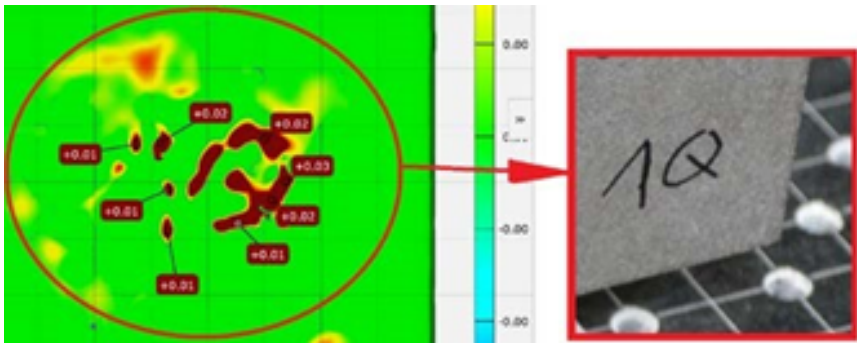

Fig. 6. The thickness of the indelible marker (used for marking the steel plates) was restricted within the range of 0.01 mm to 0.03 mm; the accuracy of the 3D scanner was sufficient to capture every detail

Preparation and performance of measurements

Preparation for scanning involved the setting of the cameras, the positioning of the rotating table, the setting of the robot, the fixing of an object to be measured (Fig. 7 and 8) and the generation of data in the STL format. The software programme used during scanning was ATOS Professional 2017.

The setting of the appropriate exposure of the cameras was followed by the adjustment of scanning parameters, i.e. the greater number of points and the faster performance of scanning. The "more points" mode enabled the recording of a greater number of points resulting from the greater permissible movement of the sensor (0.2 pixels). Measurements in the above-named mode are encumbered with a greater error, yet the scanner is insensitive to surrounding conditions (e.g. air movement) and less sensitive to surface reflexivity. Because of the simple geometry of the specimen it was possible to use the "fast scan" mode decreasing the time of a measurement by reducing the number of recorded points. Two measurement times reduced the number of reflections on scans. The application of the above-presented settings resulted in the quickening of the scanning process, the unnecessity of time-consuming pre-scan surface preparation and the lack of "holes" in obtained scans.

Before measurements, the specimen was fixed using a clamp. To ensure basing repeatability, an additional element (screwed into the rotating platform) was used. One specimen was scanned two times, where the second scan was necessary to represent geometry covered by fixing elements. Afterwards, obtained scans were put together, where the scan superposition deviation not exceeded 0.01 mm. The duration of optimised scanning in relation to the first position of the specimen amounted to 225 seconds. The scanning in the second position lasted 100 seconds, which resulted from the reduced number of robot movements, entailing the reduced number of scans necessary for the obtainment of the entire geometry. To quicken measurements after surfacing, the specimens were fixed, using plasticine, at two opposite corners and, using a two-sided adhesive tape, in the centre. After scanning, the specimen was turned around and the plasticine was placed at the corners scanned in the first position. As a result, it was possible to obtain the same scanning time for both sides. The aforesaid time amounted to 100 seconds/side (Table 3). A disadvantage of the above-presented solution was the greater number of "holes" (areas without information) on the edges. The holes were sealed up using the GOM Inspect creator and the mesh editing module.

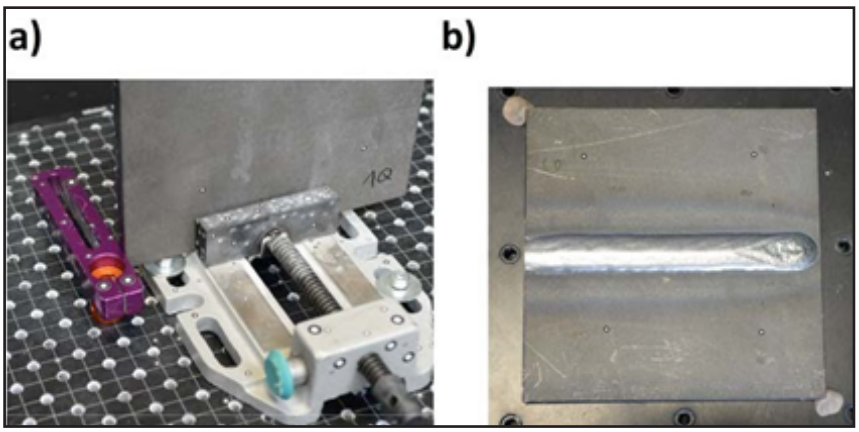

Fig. 7. Methods of attachment: a) clamp and guide element, b) attachment using tape and plasticine

Fig. 8. GOM ATOS ScanBox series 6 during the 3D scanning of the object

Table 3. Varying scanning times in relation to the method of attachment

Attachment	Before surfacing		After surfacing	
Specimen side	1	2	1	2
Scanning time, s	225	100	100	100

Programming the robot

The robot was programmed offline, using an appropriate VMR module in the GOM ATOS Professional 2017 software programme. The VMR module is a virtual measurement room being the central control station and, at the same time, measurement planning software. The operator does not need to possess special skills to programme the robot as, before a measurement, all of the robot movements are simulated and checked for safety in the virtual measurement room. The first measurement was performed to determine and optimise the robot trajectory. During the first scanning, the objective was to capture the highest possible number of reference points located on the rotating table and on the vice so that, during the following scans, the object could be oriented in space and enable the matching of successive scans.

Comparison with CAD data

Before surfacing, the mesh was entered as a CAD model into the GOM ATOS Professional 2017 software programme. After surfacing, the mesh was compared with the CAD model. Parameters subjected to verification (comparison) were the CAD surface and the mesh. The foregoing was followed by the creation of one symmetric cross-section between two edges of the specimen and two inspection cross-sections (cross-sectional slices) located 30 mm away from the specimen centre (Fig. 9).

Analysis of results

To identify the effect of a surface-accompanying heat input on the distortions of the specimens made in steel S960QL, the models were analysed for angular distortions on the basis of the cross-section containing the greatest specimen distortions and three cross-sections located in the symmetry axis of the specimens and 30 mm away from the symmetry axis, on both sides (Table 4).

Effect of the heat input on distortions in specimens

Values related to each cross-section were averaged (Fig. 10). Correlations between distortions in the specimens and heat input value were very similar in relation to all of the cross-sections.

The highest distortion was obtained in relation to a heat input of 4.28 kJ/mm, whereas the lowest distortion was obtained for a heat input of 1.76 kJ/mm. The course of distortion-related correlations was not monotonically increasing. In relation to a heat input of 1.31 kJ/mm

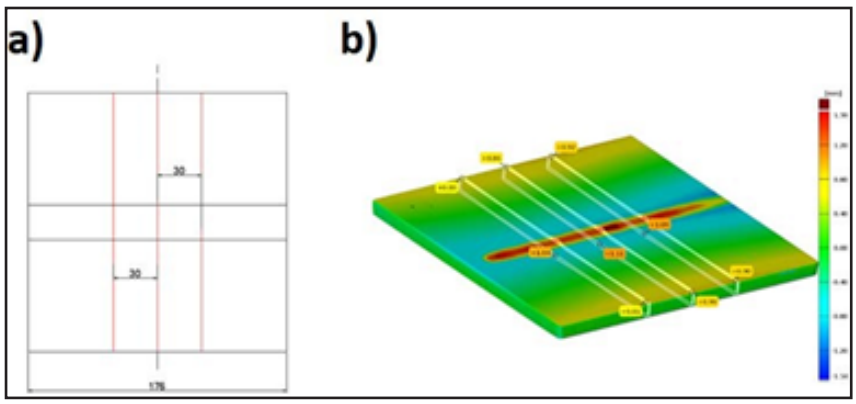

Fig. 9. Cross-sectional slices of measured data (a) and the coloured surface defect map (b)

Table 4. Effect of heat input on angular distortion in specimens.

Specimen no.	Cross-section with the maximum value of distortion, mm	Cross-section 1, mm	Cross-section 2, mm	Cross-section 3, mm
1	2.06	1.85	2.01	2.01
2	1.98	1.96	1.94	1.86
3	1.04	0.96	1.03	0.99
4	1.82	1.66	1.78	1.81
5	1.94	1.84	1.92	1.94
6	0.94	0.87	0.94	0.89
7	1.68	1.41	1.57	1.66
8	1.67	1.59	1.63	1.67
9	1.64	1.57	1.59	1.57
10	2.78	2.74	2.76	2.77

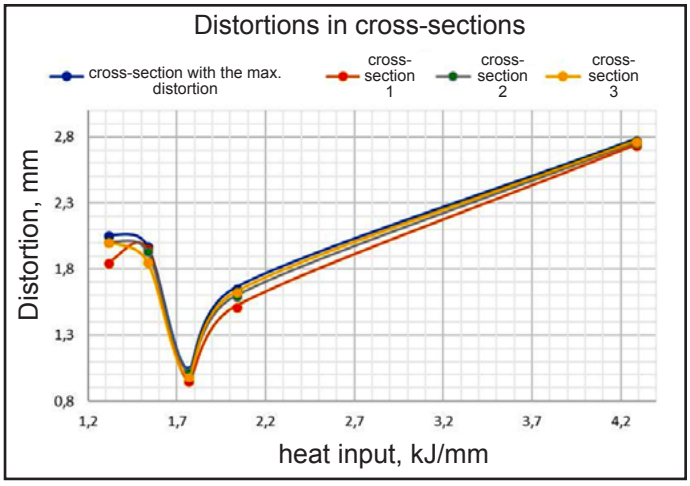

Fig. 10. Effect of heat input on welding deformations

and that of 1.53 kJ/mm, the values of distortions were higher than that in relation to a heat input of 1.76 kJ/mm. The value of distortions fell rapidly within the heat input range of 1.53 kJ/mm to 1.76 kJ/mm.

Next, distortion values grew rapidly within the heat input range of 1.76 kJ/mm to 2.03 kJ/mm. However, near the upper limit of the above-named range, the values of distortions were lower than those related to a heat input of 1.31 kJ/mm and that of 1.53 kJ/mm. The exceeding of a heat input of 2.03 kJ/mm was accompanied by the further increase in distortions, yet the course of the correlation was gentler. However, it should be noted that, because of the significant difference between the last two heat input values, it was not possible to unequivocally identify the course of the correlation in the above-named range, for instance, whether the aforesaid course was more gentle directly after exceeding a heat input of 2.03 kJ/mm or in relation to higher heat input values. The course of the correlation indicated that there was a narrow heat input range, in relation to which it was possible to obtain small angular distortions. In relation to the above-named steels, both low and high heat inputs are not favourable as they lead to significant distortions. The lowest distortions are obtainable within the heat input range of 1.7 kJ/mm to 1.8 kJ/mm.

Effect of preheating on distortions in the specimens

Specimens 4, 5 and 6 were preheated up to a temperature of 100°C. The specimens were subjected to surfacing using the same surfacing parameters as those applied when surfacing specimens 1, 2 and 3 (Fig. 11). The correlations between distortions and the heat input in relation to the specimens subjected to preheating and those not preheated were similar. Only in relation to the third cross-section, where the heat input amounted to 1.53 kJ/mm, the distortion of the preheated specimen was greater than that of the specimen not subjected to preheating. In relation to the remaining heat input values, in all of the cross-sections the distortions in the preheated specimens were characterised by lower values than in those not subjected to preheating.

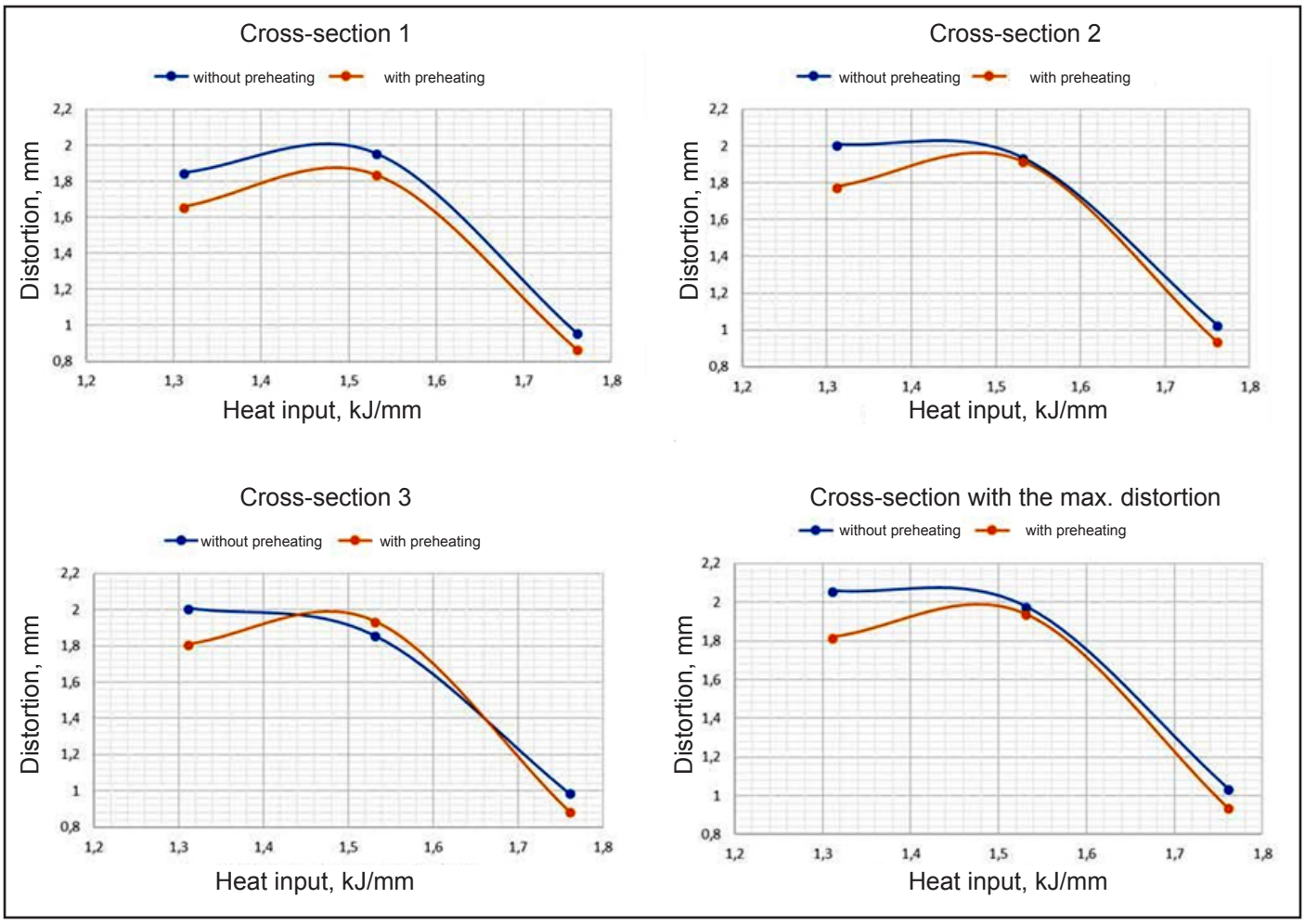

Fig. 11. Effect of preheating on welding distortions in the cross-sections of the not preheated and preheated specimens

Conclusions

The tests revealed that there is a narrow range of a heat input, in relation to which welding imperfections are significantly smaller than in relation to the remaining heat input values. The correlation between a heat input to the material during surfacing and surfacing parameters is non-linear. The range of optimum welding parameters can be determined by preparing elements using variable welding parameters and scanning obtained specimens using a 3D scanner and analysing sizes of distortions. Preheating is an effective method minimising the sizes of welding distortions, yet it should be applied with care because of the risk of an excessive heat input to the material, which could result in higher values of distortions. Three-dimensional scanning is a very useful and developmental method making it possible to monitor and analyse sizes of welding imperfections.

References

[1] Ems-usa.com [online, accessed: 1.08.2018] https://www.ems-usa.com/tech-papers/3D%20Scanning%20Technologies%20.pdf

[2] 3D scanning technologies - Aniwaa.com. [online, accessed: 1.08.2018. https://www.aniwaa.com/3d-scanning-technologies-and-the-3d-scanning-process/

[3] Huang F., Klette R., Scheibe K.: *Panoramic Imaging: Sensor-Line Cameras and Laser Range-Finders*. Wiley, 2008. https://doi.org/10.1002/9780470998267

[4] Vosselman G., Maas H.: *Airborne and Terrestrial Laser Scanning*. Whittles Publishing, 2010.

[5] FARO: 3D Measurement, Imaging & Realization Technology. [online, accessed: 8.08.2018] https://www.faro.com/

[6] Allard P., Lavoie J.: *Differentiation of 3D*

scanners and their positioning method when applied to pipeline integrity. EITEP Institute, 2014.
[7] *Precise Industrial 3D Metrology*.[online, accessed: 1.08.2018] *http://www.gom.com/*
[8] Creaform3d.com [online, accessed: 8.08.2018] *https://www.creaform3d.com/*
[9] *ZF-Laser – Lasermesstechnik*. Zf-laser.com [online, accessed: 8.08.2018] *https://www.zf-laser.com/*